VI International Conference on Computational Methods in Marine Engineering
MARINE 2015
F. Salvatore, R. Broglia and R. Muscari (Eds)

INFLUENCE OF THE EXCITATION FORCE ESTIMATOR METHODOLOGY WITHIN A PREDICTIVE CONTROLLER FRAMEWORK ON THE OVERALL COST OF ENERGY MINIMISATION OF A WAVE ENERGY CONVERTER

Francesco Ferri*, Simon Ambühl* AND Jens P. Kofoed*

*Department of Civil Engineering
Aalborg University
Sofiendalsvej 11, Aalborg, Denmark
e-mail: ff@civil.aau.dk

Key words:

Abstract. A large amount of energy is freely roaming around the world each day, without us being able to exploit it: wave energy is a largely untapped source of renewable energy, which can have a substantial influence in the future energy mix. The reason behind the inability of using this free resource is linked to the cost of the energy (CoE) produced from the different wave energy converters (WEC). The CoE from the different WECs is not yet comparable with other energy resources, due to a relative low efficiency coupled with the high structural costs. Within the sector a large effort has been addressed to optimize the WEC efficiency by means of different control strategies. In several articles [1, 2], it has been shown that with simple modifications of the control law, the absorbed energy can be doubled or quadrupled. Whilst the improvement of the efficiency will increase the revenue of the machine, the application of an advance control strategy will most probably increase the loads exerted on the structure, leading to an increment of the structural cost. Therefore, the problem of minimising the CoE produced by a WEC is at least a 2D problem. In a previous article [3], the minimisation problem has been investigated with a sequential approach, and the results have been reported for different control strategies. The Model Predictive Controller (MPC) seemed to have superior performance in terms of energy maximisation and loads on the structure, leading to a minimal CoE. But as presented in [3] the MPC was implemeted with perfect knowledge of the future load time series, which is physically not achivable. This article is an extension of the work presented in [3] with a closer focus on the influence of the excitation force prediction on the capability of the MPC architecture. Different estimator models of the excitation force time series are benchmarked, and validated with laboratory results.

1 INTRODUCTION

Due to its intrinsic potential, the wave energy sector has been the focus of researches since the seventies, years in which the modern wave sector movement started. From those years many concepts have been idealised and nowadays few of them reached a pre-commercial stage. Nevertheless, as presented in [4], the cost of energy (CoE) limits the sector to become a competitor of others, and more mature, renewable energy technologies.

The simplest approach to reduce the CoE works on the maximisation of the efficiency of the machine. As firstly presented in [5], the maximisation of the absorbed energy can be obtained by changing the load exerted by the power take off system (PTO) on the oscillating body. If for some fraction of the wave cycle some energy is fed into the oscillating body, the efficiency of the device can be increased over a wide spectrum of sea states. This last class of controllers is commonly known as active control, while if no energy feed back is allowed the controller is commonly called passive. A summary of the different available alternatives is reported in [6, 2].

From a theoretical point of view, the active controllers are capable to increase the energy yield of the wave energy converter (WEC) by a factor two or four if compared with a simpler passive controller. Though, their applicability in real life has only been little proven due to shortcomings, such as non-linearities handling, short-term load forecast requirements, etc.

Working on the control algorithm is a rather straightforward method to minimise the CoE, but whether or not the maximisation of the efficiency leads to a true minimum of the CoE, it has not been proven yet. In fact, as introduced in [3] the maximisation of the energy can lead to a local minima in the CoE minimisation problem, because the increased yield is paired with an increased mean load level, which in turn affect the structural design of the WEC through its fatigue limit state. Since the structural costs of the WEC are of utmost importance in the overall CoE, it is straightforward to understand the need for a multivariate optimisation algorithm.

The work presented in this document is a continuation of the work discussed in [3]. In short, the article presented a sequential approach for the bivariate optimisation of the CoE, as depicted in Fig. 1

The main outcome of the article was: for a single degree of freedom WEC of the point absorber type, the model predictive control (MPC) is the best alternative from an economic perspective. But the implemented model relied on severe assumptions. The first, and probably the most important, is the perfect knowledge of the future wave load exerted on the structure. Since the MPC optimise the control trajectory based on a short-time prediction of the system dynamic, it is easy to see that the methodology used to predict the wave loads will have a major impact on the controller results.

Therefore, the objective of this study is to investigate the influence of the prediction algorithm on the performance of the MPC and compared the results with an ideal model with full knowledge of the future loads. The results are reported in terms of absorbed

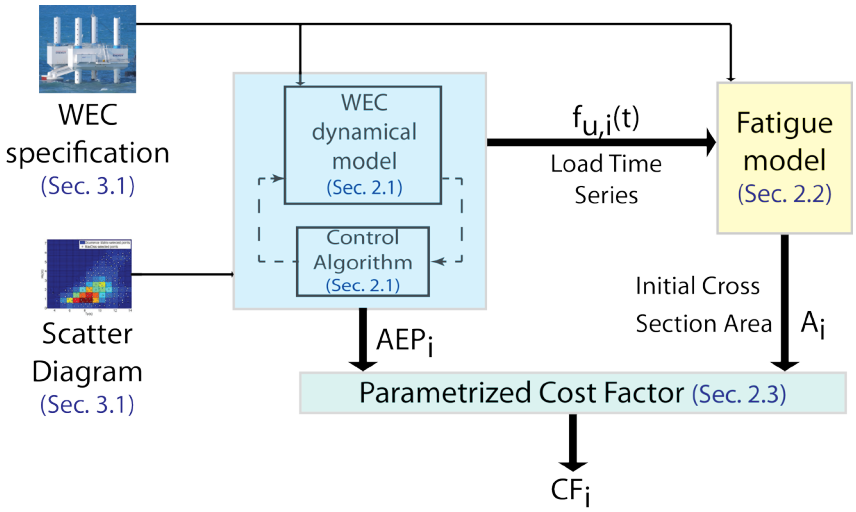

Figure 1: Work flow diagram of the proposed methodology. Subscript "i" refers to the ith-control strategy and Ω defines the set of the selected control strategies.

power, cross section area of specific details and CoE. The analysis is carried out for a single degree of freedom WEC of the point absorber type. The same approach can be extended for other WECs of the wave activated body types, whilst the implementation of the model for oscillating water columns or overtopping WECs is not straightforward.

The work presented in this article is organised as follow. There is a first short introduction of the problem (Sec. 1), followed by a description of the theoretical background (Sec. 2), where the MPC and the forecast methodologies are detailed. Then, the results of the applied theory are reported and discussed for the specific case study (Sec. 3), followed by a short conclusion (Sec. 4).

2 METHODS

2.1 Numerical Model and Control

Considering a single degree of freedom WEC of the point absorber type, the dynamic of the system excitated by the passing waves can be described by the Cummin's equation [7]; an integro-differential equation based on the Newton's second law:

$$(M + a_\infty)\ddot{x}(t) + \int_{-\infty}^{t} h_{rad}^{\dot{x}}(t-\tau)\dot{x}(\tau)d\tau + K_h y x(t) = f_u(t) + \int_{-\infty}^{\infty} h_{ex}^{\eta}(t-\tau)\eta(\tau)d\tau \quad (1)$$

Here, M is the mass of the system, a_∞ is the added mass at infinity frequency, $x(t)$ is the displacement of the body and the over-dot is used to represent the order of the time derivative, $h_{rad}^{\dot{x}}$ is the impulse response function (irf) that maps the body velocity into the radiation force, K_{hy} is the hydrostatic stiffness, f_u is the control load and h_{ex}^{η} is the irf that maps the surface elevation (η) into the excitation force. The time dependency of any variable is represented by the term (t). Both integrals represent a convolution integral.

The interaction between water, waves and body can be dealt with three contributions

Excitation force represents the force exerted by the passing wave on the structure held at the equilibrium position.

Radiation force represents the force acting on the body due to motion of the body in otherwise still water.

Hydrostatic stiffness represents the force acting on the body due to the gravitational load and the buoyancy.

In a simplistic approach the aim of the controller is to maximise the average absorbed power ($\overline{P}$) that is the mean of the product between the control load and the body velocity:

$$\max_{f_u} \quad \left(\overline{P} = \frac{1}{T} \int_0^T f_u(t)\dot{x}(t)dt \right) \tag{2}$$

where T represents the time windows for the maximisation.

Since the scope of the article is the investigation of the influence of the prediction methodology into the performance of a MPC, a short description of the controller is given hereafter; for a comprehensive list of controllers type one could refer to [6, 2].

The MPC is a digital control technique that evaluate the optimal control trajectory based on a given cost function over a finite horizon. The MPC has been only recently implemented in the control of WECs and for a full description of the MPC model the reader can refer to the following works [8, 1, 9, 10, 11, 12].

The controller solves a possible constrained optimisation problem based on the actual state of the system, a number N of projected future states and the course of external inputs over the control horizon. The projection of the actual state over the prediction horizon is achieved by using a dynamic model of the system. The external inputs are the control force and the excitation force; they are listed in (1) on the right hand side of the equation. The cost function is optimised at each time sample and a new control trajectory for the whole horizon is assessed. Using the receding horizon control principle only the first sample of the control trajectory is effectively fed into the system. This gives the ability to react to an unforeseen disturbance. Two different implementations of the MPC are available in literature for WECs, which differ for formulation of the cost function:

- Direct implement the objective of maximum average power into the cost function
- Implement a tracking reference objective function

In this work, the first kind of implementation has been chosen, and in particular the work described in [1]. The cost function is the absorbed average power as presented in (2), where T is equal to the control horizon and the actual time is zero.

2.1.1 Excitation force prediction

In order to maximise the objective function the excitation force needs to be defined for the full prediction horizon. The information available is the excitation force from the actual instant of time ($f_{ex}[k]$) to any past instant ($f_{ex}[k-i]$). In order to keep the analysis focused on the influence of the prediction strategy only, it has been assumed that the excitation force is a measurable quantity and therefore its value at the actual instant k is known without error. In general this assumption is not true and a soft-sensor (observer) needs to be used. Then the observation error should be combined to the prediction error to obtain the overall error.

Based on the available literature, three different strategies have been used and they are described hereafter.

Autoregressive Model In an autoregressive (AR) model it is assumed that the variable can be predicted using a linear combination of the past value of the variable, [13, 14, 10]. Therefore, the one-step ahead predictor can be defined as:

$$\hat{f}_{ex}[k+1|k] = \sum_{i=0}^{N-1} a_i \cdot f_{ex}[k-i] \tag{3}$$

Here, $\hat{f}_{ex}[k+1|k]$ is the predicted excitation force at time $k+1$ given the state of the variable at time k, N is the model order, $a_i[k]$ are the model coefficients and $f_{ex}[k-i]$ is one entry in the vector containing the past values of the excitation force. The model coefficients are time-dependent but in general their dependency in time is loose. In this work it has been chosen to change the AR model for each sea-state, as a compromise between accuracy and computational time. The coefficients of the AR model are assessed by minimising in the least square sense the error between the predicted and a given time series as:

$$\min_{a_i} \quad \left[\sum_j \left(\hat{f}_{ex}^j - f_{ex}^j \right)^2 \right] \tag{4}$$

The multi-step ahead prediction can be obtained using the plug-in or sequential method, in which the previously predicted step $(k+1)$ is prepended at the vector of past values of the excitation force.

Cyclical Model In this method the excitation force is expressed as a superposition of a number m of linear harmonic components, [14, 15]. The choice of m and the distribution of the harmonics within the wave spectrum is a critical point as discussed in [14, 15]. Assuming the index i ranging from 1 to m the model can be expressed as:

$$\begin{bmatrix}\psi_i[k+1]\\ \psi_i^*[k+1]\end{bmatrix} = \begin{bmatrix} cos(w_i\Delta T) & sin(w_i\Delta T)\\ -sin(w_i\Delta T) & cos(w_i\Delta T)\end{bmatrix}\begin{bmatrix}\psi_i[k]\\ \psi_i^*[k]\end{bmatrix} + \begin{bmatrix}\xi_i[k]\\ \xi_i^*[k]\end{bmatrix} \tag{5}$$

$$f_{ex}[k] = \sum_{i=1}^{m}\psi_i[k] + \zeta[k] \tag{6}$$

The cyclical model can be conveniently reshaped into a canonical state-space from, where the state matrix is a block diagonal matrix composed by the m harmonics matrices, and the output matrix perform the summation over the first element of the state vector for each harmonic. A linear Kalman filter can be used on the model to obtain the best linear estimation of $\hat{f}_{ex}[k|k]$, see [16].

From the estimation of the excitation force, the multi-step ahead prediction can be obtained through the free evolution of the model.

Cyclical Model with variable frequency In order to overcome the problem of the selection of m and the harmonic distribution, it is possible to consider the frequency as a variable and add it to the state vector [14, 15]. The excitation force is now defined by a single cyclical model as:

$$\begin{bmatrix}\psi_i[k+1]\\ \psi_i^*[k+1]\\ \omega[k+1]\end{bmatrix} = \begin{bmatrix} cos(\omega[k]\Delta T) & sin(\omega[k]\Delta T) & 0\\ -sin(\omega[k]\Delta T) & cos(\omega[k]\Delta T) & 0\\ 0 & 0 & 1\end{bmatrix}\begin{bmatrix}\psi_i[k]\\ \psi_i^*[k]\\ \omega[k]\end{bmatrix} + \begin{bmatrix}\xi_i[k]\\ \xi_i^*[k]\\ \kappa[k]\end{bmatrix} \tag{7}$$

$$f_{ex}[k] = \psi_i[k] + \zeta[k] \tag{8}$$

Since the model became non-linear the estimation of the excitation force at the time k needs to be evaluated using the Extendend Kalman filter, see [16]. The multi-step ahead prediction is obtained through the free evolution of the non-linear model.

2.2 Fatigue Assessments

Fatigue failure is an important failure mode of offshore structures and expectably even more for WECs where the resonance condition is sought. For estimating the fatigue of a structural part, the SN curve together with Miner's rule [17] is used here. SN curves for offshore applications can be found in [18]. Miner's rule uses sequence independent linearised damage accumulation and assumes that fatigue failure occurs when [17]:

$$\sum_{k=1}^{N_k}\frac{n_k}{N_k} = 1 \tag{9}$$

where N_k is the total number of cycles of a given stress range leading to fatigue failure and n_k the expected number of cycles at the same stress range during the life-time of the WEC. The SN curve shows the number of cycles leading to fatigue failure of a given stress

amplitude. When using the SN approach, a linear or bilinear formulation, where plastic deformation is allowed, can be implemented. Rain-flow counting (see [19]) can be used to discretise the load time series into groups/intervals of load amplitudes. A certain interval k has n_k cycles per year of a certain load range ΔQ_k (e.g. normal force). It is assumed that the stress range $\Delta\sigma_k$ can be expressed by a design parameter z (e.g. cross section area) and the corresponding load range ΔQ_k:

$$\Delta\sigma_k = \frac{\Delta Q_k}{z} \tag{10}$$

The bilinear SN curve has a slope change at $\Delta\sigma_D$ where the number of cycles to failure N_D is equal to 10^6:

$$\begin{aligned} N &= K_1 S^{-m_1} \quad \text{for} \quad S \geq \Delta\sigma_D \\ N &= K_2 S^{-m_2} \quad \text{for} \quad S < \Delta\sigma_D \end{aligned} \tag{11}$$

where $K_{1,2}$ are the stress intensity factors, and $m_{1,2}$ are the crack growth parameters. A design equation can be used to calculate the design equation parameter z and can be written for a bilinear approach using Miner's rule as, see e.g. [20]:

$$1 - \underbrace{\sum_i \sum_j \sum_{k_1} \frac{T_{FAT} n_{ijk_1}}{K_1^c} s_{ijk_1}^{m_1} P(H_{m0_i}, T_{P_j})}_{S \geq \Delta\sigma_D} - \underbrace{\sum_i \sum_j \sum_{k_2} \frac{T_{FAT} n_{ijk_2}}{K_2^c} s_{ijk_2}^{m_2} P(H_{m0_i}, T_{P_j})}_{S < \Delta\sigma_D} = 0 \tag{12}$$

where $\log(K^c)$ is the characteristic value of $\log(K)$, n_{ijk} is the number of stress ranges per year given the significant wave height H_{m0_i} and the wave peak period T_{P_j}, $s_{ijk} = \Delta Q_{ijk}/z$ is the stress range ijk given H_{m0_i} and T_{P_j}. The fatigue design life T_{FAT} is equal to $FDF \cdot T_L$ with fatigue design factor FDF and design life time T_L. The joint probability of H_{m0_i} and T_{P_j} is equal to $P(H_{m0_i}, T_{P_j}) = P(H_{m0_i}) P(T_{P_j} | H_{m0_i})$ and indicates the probability of occurrence of a certain sea state.

2.3 Cost Factor

This section focuses on bringing together the influence of a certain control strategy on harvested energy, which will define the income during lifetime, and the resulting structural design which drives the investment costs. In order to compare different control strategies, a simple economical model is used.

From a certain structural detail, one can hardly comment on the control strategy's overall cost impact. But one can, based on some simple assumptions get an idea of the relative impact of the different control strategies on the overall cost.

It is assumed that the total lifetime costs consists of one part, which is dependent on the control strategy (called $C_1(i)$, mainly cost for PTO and structure of PTO arm) and other investment costs (called C_2, e.g. platform, or electricity connection to shore), which are assumed to be constant for all control strategies. The control dependent costs are assumed to be proportional to the cross sectional area of a certain critical structural

component. The cost factor $CF(i)$, which shows the ratio between total investment costs and the annual energy production ($AEP(i)$), for a given control strategy i can be written as:

$$CoE(i) = \frac{C_1(i) + C_2}{AEP(i)} = \frac{p\frac{A_c}{A_{ref}} + (1-p)}{AEP(i)} \cdot C_{ref,tot} \tag{13}$$

$$CF(i) = \frac{p\frac{A_c}{A_{ref}} + (1-p)}{AEP(i)} \tag{14}$$

where $C_{ref,tot}$ is the total lifetime cost of a certain design with a reference control strategy, A_{ref} the cross sectional area of a critical structural component for the reference control strategy, $A(i)$ the resulting cross sectional area of control strategy i and p represents the percentage of the total lifetime costs, which are dependent on the control strategy. Even though the main assumption adopted - linear relation between WECs cost and structural dimensions - is rather stringent, the cost factor can still give a valuable tool to gain insight into the economic potential of a WEC and afterwards ease the comparison between proposed concepts.

3 RESULTS AND DISCUSSION

3.1 Case Study Description

In line with the choice performed in [3] the WEC selected for the analysis is the Wavestar WEC. The Wavestar is a multi point absorber WEC. The prototype shown in Fig. 2 is a sub-section of the full machine, it consists of four piles and two floaters as well as a platform where the mechanical and electrical devices are stored. The floaters, which are excited by the passing waves drive a hydraulic system which impels a turbine and a generator. The Wavestar device was installed in 2009 and fed electricity into the grid until it was moved to the harbour for reconfiguration in September 2013.

Site Assessement Sea state measurements over a period of 6 years are provided by [21], based on recordings from a buoy (6332100N, 474700E, water depth: 17 m) located near the Wavestar device. The dataset contains the frequency domain wave parameters, significant wave height (H_{m0}) as well as the peak period (T_P), measured with a time interval of 3 hours. The resulting probability of occurrence of different wave states are shown in Tab. 1 and are used in this case study.

Numerical Model of the Wavestar WEC The prototype scale of the Wavestar WEC was used to perform the numerical analysis. In addition only one floater was considered, resulting in single degree of freedom system. The model introduced in (1) is used to describe the dynamic response of the system. Tab. 2 summarises the model parameters used in this case study.

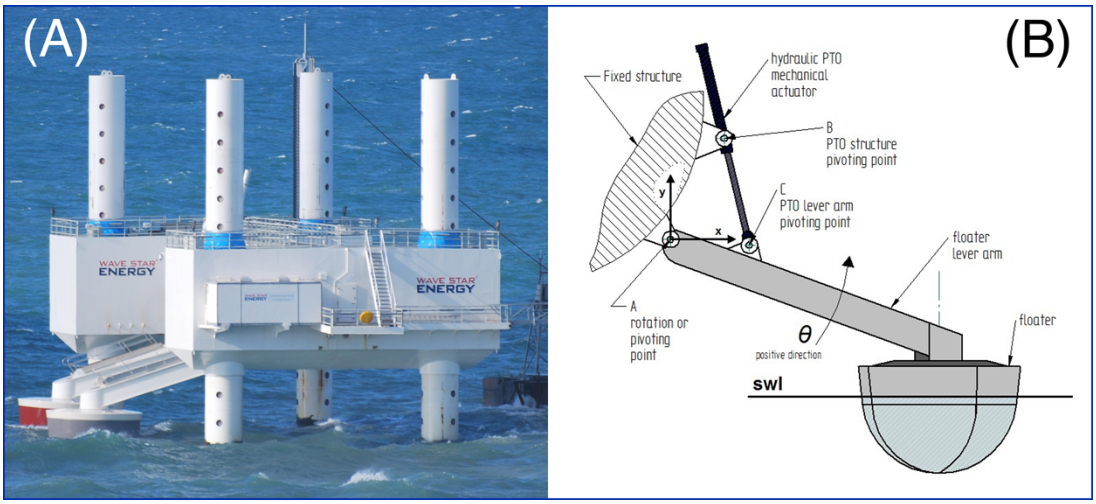

Figure 2: (A) Wavestar prototype at Hanstholm (DK), (B) Sketch of floater details with main components and coordinate system.

Table 1: Relative occurrence of different wave states from 6 years, buoy measurements ($[H_{m0}]$=m, $[T_P]$=s). Both parameters defines the mean value over an interval. The adopted discretisation is 1 s in T_p and 0.5 m in H_{m0}.

H_{m0}/T_P	0.5	1.5	2.5	3.5	4.5	5.5	6.5	7.5
0.25	-	-	-	0.04	0.04	0.02	0.01	-
0.75	-	-	-	0.07	0.17	0.11	0.05	0.01
1.25	-	-	-	-	0.06	0.11	0.05	0.01
1.75	-	-	-	-	-	0.06	0.05	0.02
2.25	-	-	-	-	-	0.01	0.05	0.02
2.75	-	-	-	-	-	-	0.01	0.02
3.25	-	-	-	-	-	-	-	0.01

For each sea state described in Tab. 1, a surface elevation time series of 3 hours is fed into the numerical model.

The White Noise filtering technique is adopted to generate the surface elevation time series. The filter uses a JONSWAP spectral model [22] with peak enhancement factor (γ) equal to 3.3 and a sample frequency equal to 20 Hz.

In [3] the time series length was set to 10x3 h, in order to reduce the statistical uncertainty of the model input. Due to the high computational time of the MPC with constraints, it was decided to investigate the evolution of the variance of the results as a function of the time series length, following the approach described in [23]. Fig. 3 summarises the results of the analysis, from which it has been chosen to reduce the sample time to 3 h.

The linear hydrodynamic coefficients as well as the hydrostatic stiffness coefficients have

Table 2: Model parameters for the Wavestar WEC.

		Hydrostatic and structural parameters	
Moment of Inertia	J_{st}	2.45·1e6	$[kgm^2]$
Hydrostatic Stiffness	K_{hy}	14.0·1e6	$[Nm/rad]$
Maximum exerted moment	M_{max}	1.0·1e6	$[Nm]$
Drag Coefficient	C_D	0.25	$[--]$
PTO stroke	S_{PTO}	2.0	$[m]$
Natural Period in Pitch	T_n	∼3.5	$[s]$
		Hydrodynamic model parameters	
Added mass at infinity frequency	a_∞	1.32·1e6	$[kgm^2]$
Radiation Moment TF numerator	a_{RAD}	[4.93, 1.08]·1e6	$[--]$
Radiation Moment TF denominator	b_{RAD}	[1, 2.56, 5.16]	$[--]$
Excitation Moment TF numerator	a_{EX}	[5.4e10, 2.7e12]	$[--]$
Excitation Moment TF denominator	b_{EX}	[3.6e4, 3.9e5, 1.5e6, 2.6e6, 1.6e6]	$[--]$

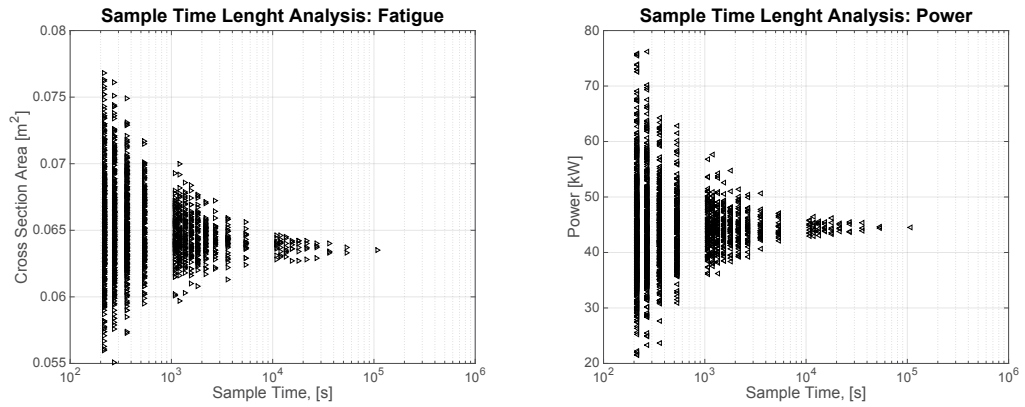

Figure 3: Investigation of the influence of the time series length on the results. Left: variation of the cross section area. Right: variation of the mean absorbed power.

been evaluated using a commercial BEM solver [24]. The radiation frequency functions have been interpolated with a rational polynomial approximation, whose order is reduced using the Hankel singular value, [25]. The resultant second order transfer function is listed in Tab. 2.

The AR model used in the work has an order of 80. The order was selected based on the goodness-of-fit (GOF) as introduced by [14, 13]. It should be noticed that the GOF was much in line with the results reported in [13], with a value always below 60 % for the required prediction horizon. On the contrary, as reported in [14] the AR model seems to be able to have better performances and further investigations are need in order to clarify this point.

The cyclical model used in the work is a simplified version of the one presented in the

previous section. In fact, the model only uses a frequency that is determined by the peak period of the specific sea-state. Adding other frequencies, nor changing their distribution showed any performance improvements. In line with the results presented in [14], the GOF of this method is below the one of the AR model, being always below 50 %. In addition, it should be noticed that the model is highly sensitive to the Kalman filter parameters, which has been roughly estimated based on a sensitivity analysis.

The non-linear cyclical model showed the same sensitivity of the previous model to the Extended Kalman Filter parameters. The non-linear model performs worst than the linear model; the GOF is always below 20 %.

3.2 Case Study Results

The MPC used on this work uses a prediction horizon of 120 samples, which results in a forecast of 6s. The selection of the prediction horizon length is a result of the trade off between performances of the controller and computational time. Fig. 4 shows the relation between the mean absorbed power and the prediction horizon length (H) for different angular frequencies of the incoming waves. The mean absorbed power is normalised by the maximum value in the dataset.

In general, it can be seen that there is an important performance step from the case with H=80 and the case with H=120, while the variation of the performance flattens-out for the following cases. Further, the lower is the angular frequency the higher is the fork between the different cases. In fact, as the wave period grows the prediction horizon cover less and less of a full wave cycle, resulting in a poorer performance. As a rule of thumb it seems clear that the prediction horizon should be has long as the longest wave period in the scatter diagram, or at least to the longest with statistical relevance. For the specific case study, the statistical relevance of the cases with Tp = 7.5 s is relatively low, and therefore a higher error is acceptable in those simulated sea-states.

Fig. 5 summurise the results for the AEP and the cross section area as a function of the different prediction algorithms. The following acronyms are used in the following:

- MPC - MPC with perfect prediction algorithm, this is the reference point for the other MPC implementations
- MPC-AR - MPC with autoregressive model.
- MPC-CyKF - MPC with linear cyclical model
- MPC-CyEKF - MPC with non-linear cyclical model

In addition to these implementations, the results for a proportional (P) passive controller and for a proportional and integral (PI) active controller are reported too. For more details about these two controllers see [3].

In the figure the AEP is represented with blue bars and the cross section area with yellow bars. As expected, the prediction error affects negatively the power performances

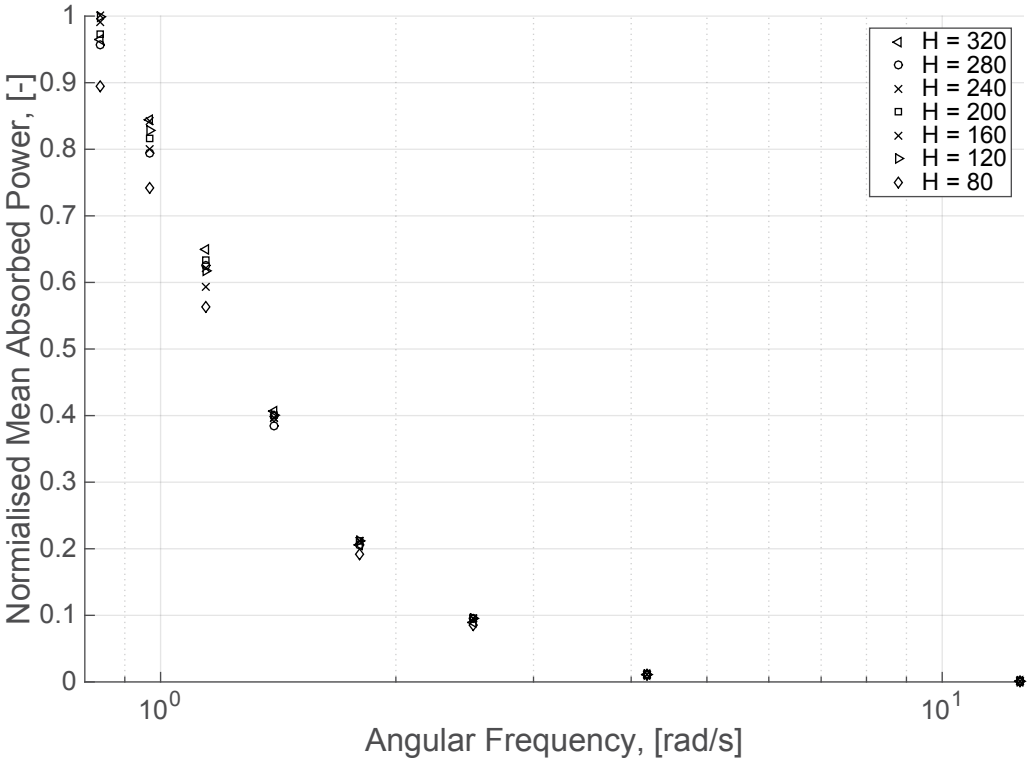

Figure 4: Investigation of the influence of the prediction horizon length on the power performance of the MPC, as a function of the frequency of the incoming waves.

of the MPC, even though it seems that the reduced power is paired with a reduced load level. It is important to notice that when the prediction error is too high the performance of the MPC is getting closer to the one of the P controller. A closer look to this result showed that the behavior of the MPC react to the wrong prediction by drastically reducing the active power fed into the system and reverting to a simple passive controller.

Fig. 6 shows the previous results combined into the CF model presented in (14). The CF is normalised by the CF of the P controller in line with the choice done in the previous work. For each controller type the p parameter has been changed in the range 0-20 %, on order to assess the sensitivity of the CF to the unknown p parameter. The red line represents the mean value, the blue box represents the 25-75 % percentile and the whisker represents the maximum and minimum acceptable values. Any outlier has been removed from the dataset. For the P control there is no variation on the results because it has been chosen as the normalisation point.

For the other controllers the influence of p is quite limited, reducing the influence of its uncertainty. Focusing on the mean values only, it is interesting to notice that the MPC is still a valuable alternative to the PI controller even in case of an important prediction

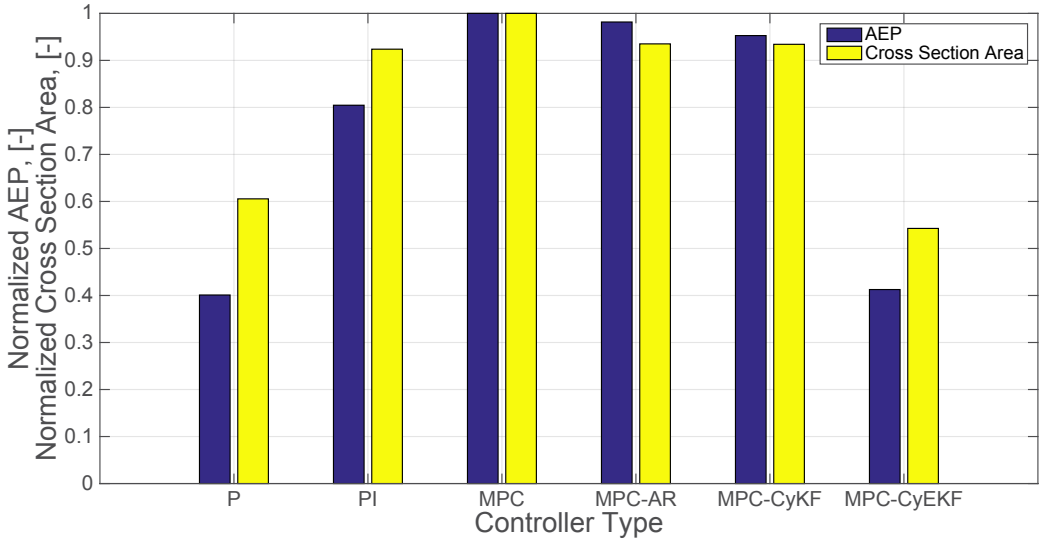

Figure 5: Comparison of the normalised cross section area (yellow) and the normalised AEP (blue) for the different control types.

error.

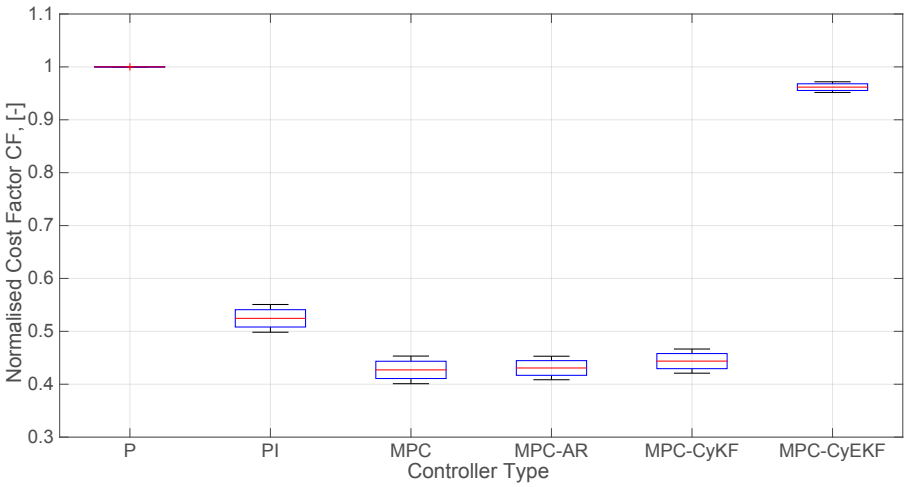

Figure 6: Variation of the normalised cost factor as a function of the different controller types. For each controller the p parameters is varied from 0 to 20%, where the red line represent the median, the box limits represent the 25 and 75% percentile and the whisker is extended to the maximun and minimum data points not considered outliers.

For the case MPC-CyEKF though the prediction error is just misleading the controller, and the whole performance is deteriorated.

It should be noticed that the prediction error grows with the distance from the actual time, while the controller, given the receding horizon scheme prioritises the near future information, and therefore the high error in the last part of the prediction horizon become negligible.

4 CONCLUSIONS

This article is the continuation of the work presented in [3], where a sequential bivariate algorithm to perform the optimisation of the CoE for a WEC was presented.

In particular the focus is given to the performance of the MPC, because in the previous work the implementation of the MPC was ideal, with perfect knowledge of the future wave load. Therefore, the influence of the prediction methodology into the resulting CF has been investigated. Three different prediction methods have been used: autoregressive model, linear cyclical model and non-linear cyclical model.

The main outcome of the analysis is that the MPC can handle a large error in the prediction methods, and when the error become too large, the MPC revert to a simple passive controller. If compared with a PI controller, the CF can be reduced by roughly 20 % and the number become 50 % if compared with the widespread passive controller technique.

Even if the better performance of the MPC needs to be balanced by the increased implementation complexity, overall the MPC seems to be a viable solution.

Two main points are still open though, which will be part of a future analysis:

- Influence of the observation of the excitation force into the overall prediction error
- Implementation of the MPC controller into a physical model of the Wavestar machine and comparison with a P and PI controller.

ACKNOWLEDGMENT

The author gratefully acknowledge the financial support from the Energy Technology Development and Demonstration Program (EUDP), under the project "WaveSpring for enhancing wave energy absorption", which made this work possible. Further, the author gratefully acknowledge Jørgen Hals for his technical support, and Morten Thøtt Andersen for the help given in writing and reviewing the article.

REFERENCES

[1] J. A. M. Cretel, G. Lightbody, G. P. Thomas, and A. W. Lewis, "Maximisation of Energy Capture by a Wave-Energy Point Absorber using Model Predictive Control," in *Proceeding of International Federation of Automatic Control - IFAC*, no. 2002, 2011, pp. 3714–3721.

[2] J. Hals, "Modelling and phase control of wave-energy converters," Ph.D. dissertation, Norwegian University of Science and Technology, 2010.

[3] F. Ferri, S. Ambühl, B. Fischer, and J. P. Kofoed, "Balancing power output and structural fatigue of wave energy converters by means of control strategies," *Energies*, vol. 7, no. 4, pp. 2246–2273, 2014.

[4] J. Weber, "Wec technology readiness and performance matrix–finding the best research technology development trajectory," in *International Conference on Ocean Energy*, 2012.

[5] D. Evans, "Power from water waves," *Annual Review of Fluid Mechanics*, vol. 13, no. 1, pp. 157–187, 1981.

[6] F. Ferri, "Wave-to-wire modelling of wave energy converters: Critical assessment, developments and applicability for economical optimisation," Ph.D. dissertation, Department of Civil Engineering, Aalborg University, 2014.

[7] W. Cummins, "The impulse response function and ship motions," DTIC Document, Tech. Rep., 1962.

[8] P. Gieske, "Model predictive control of a wave energy converter: Archimedes wave swing," Ph.D. dissertation, Delft University of Technology, Delft, 2007.

[9] J. Hals, J. Falnes, and T. Moan, "Constrained optimal control of a heaving buoy wave-energy converter," *Journal of Offshore Mechanics and Arctic Engineering*, vol. 133, no. 1, pp. 1–15, 2011.

[10] T. K. Brekken, "On model predictive control for a point absorber wave energy converter," in *PowerTech, 2011 IEEE Trondheim*. IEEE, 2011, pp. 1–8.

[11] M. Richter, M. Magaña, O. Sawodny, and T. K. A. Brekken, "Nonlinear Model Predictive Control of a Point Absorber Wave Energy Converter," vol. 4, no. 1, pp. 118–126, 2013.

[12] E. Abraham and E. C. Kerrigan, "Optimal Active Control and Optimization of a Wave Energy Converter," vol. 4, no. 2, pp. 324–332, 2013.

[13] B. Fischer and P. Kracht, "Online-Algorithm using Adaptive Filters for Short-Term Wave Prediction and its Implementation," in *International Conference on Ocean Energy, ICOE*, Dublin, Ireland, 2012, pp. 1–6.

[14] F. Fusco and J. V. Ringwood, "Short-Term Wave Forecasting for Real-Time Control of Wave Energy Converters," *IEEE Transactions on Sustainable Energy*, vol. 1, no. 2, pp. 99–106, Jul. 2010. [Online]. Available: http://ieeexplore.ieee.org/lpdocs/epic03/wrapper.htm?arnumber=5451110

[15] S. P. Becker, "V e r s i tat," Master Thesis, University of Kassel, 2014.

[16] R. G. Brown, P. Y. Hwang *et al.*, *Introduction to random signals and applied Kalman filtering*. Wiley New York, 1992, vol. 3.

[17] M. A. Miner *et al.*, "Cumulative damage in fatigue," *Journal of applied mechanics*, vol. 12, no. 3, pp. 159–164, 1945.

[18] D. N. Veritas, "Fatigue design of offshore steel structures," *DNV Recommended Practice DNV-RP-C203*, 2010.

[19] ASTM-E1049-85, "Standard practices for cycle counting in fatigue analysis." American society for testing and materials West Conshohocken, PA, 1990.

[20] S. Márquez-Domínguez and J. D. Sørensen, "Fatigue reliability and calibration of fatigue design factors for offshore wind turbines," *Energies*, vol. 5, no. 6, pp. 1816–1834, 2012.

[21] DanWEC, "Danish wave energy center," March 2015, visited on 21st March 2015. [Online]. Available: http://www.danwec.com/

[22] K. Hasselmann, T. Barnett, E. Bouws, H. Carlson, D. Cartwright, K. Enke, J. Ewing, H. Gienapp, D. Hasselmann, P. Kruseman *et al.*, "Measurements of wind-wave growth and swell decay during the joint north sea wave project (jonswap)," Deutsches Hydrographisches Institut, Tech. Rep., 1973.

[23] C. M. García, M. I. Cantero, Y. Niño, and M. H. García, "Turbulence Measurements with Acoustic Doppler Velocimeters," *Journal of Hydraulic Engineering*, vol. 131, no. 12, pp. 1062–1073, 2005.

[24] C.-H. Lee, *WAMIT theory manual*. Massachusetts Institute of Technology, Department of Ocean Engineering, 1995.

[25] T. Pérez and T. I. Fossen, "Time-vs. frequency-domain identification of parametric radiation force models for marine structures at zero speed," *Modeling, Identification and Control*, vol. 29, no. 1, pp. 1–19, 2008.